Magnetically Responsive Calcium Carbonate Microcrystals

Rawil F. Fakhrullin,* Aidar G. Bikmullin, and Danis K. Nurgaliev

Department of Biochemistry, Kazan State University, Kreml uramı 18, Kazan 420008, Republic of Tatarstan

ABSTRACT Here we report the fabrication of magnetically responsive calcium carbonate microcrystals produced by coprecipitation of calcium carbonate in the presence of citrate-stabilized iron oxide nanoparticles. We demonstrate that the calcite microcrystals obtained possess superparamagnetic properties due to incorporated magnetite nanoparticles and can be manipulated by an external magnetic field. The microcrystals doped with magnetic nanoparticles were utilized as templates for the fabrication of hollow polyelectrolyte microcapsules, which retain the magnetic properties of the sacrificial cores and might be spatially manipulated using a permanent magnet, thus providing the magnetic-field-facilitated delivery and separation of materials templated on magnetically responsive calcite microcrystals.

KEYWORDS: magnetic nanoparticles • calcium carbonate • hollow microcapsules • polyelectrolytes

INTRODUCTION

The development of novel functional materials that are based on or inspired by naturally occurring microparticles has attracted a significant amount of attention by researchers worldwide (1). In particular, biocompatible inorganic microparticles are routinely used as templates for the fabrication of hollow multilayered microcapsules using layer-by-layer (LbL) polyelectrolyte deposition (2). Among other templates, calcium carbonate microcrystals are currently regarded as a promising tool in the fabrication of biomimetic materials, which have potential applications in protein encapsulation (3) and as three-dimensional templates for the development of novel materials (4) and multicellular assemblies (cellosomes) (5). This implies the necessity to control such important factors as the size distribution, morphology, and stability of $CaCO_3$ templates. Typically, calcium carbonate exists in several crystalline polymorphs along with the amorphous phase, and these forms differ considerably in shape and thermodynamic stability (6). In living organisms, the processes of cell-controlled biomineralization lead to the synthesis of extremely stable and unusual three-dimensional calcium carbonate microparticles utilized by the host organisms as skeletons and protective shells. Remarkably, the stability of such biogenic calcium carbonate microparticles is increased by various biomacromolecules (7); therefore, several recent studies were aimed at demonstrating the influence of biomacromolecules (8) and living cells (9) on the precipitation and morphology of calcium carbonate microparticles. Obviously, the ability to spatially manipulate the calcium carbonate microcrystals using external stimuli might be a key function in the separation and transportation of the $CaCO_3$ templates themselves and the functional materials based on these templates. Currently, iron oxide superparamagnetic nanoparticles, introduced as a component in hollow microcapsules and microspheres (10), inorganic and organic nanotubes (11), microtubules (12), nanomagnetic sponges (13), hybrid organic−inorganic microgels (14) and anisotropic and Janus particles (15), provide a robust way of external manipulation using a permanent magnet, thus allowing the targeted delivery, separation, and extraction of magnetically modified materials. A similar approach was proposed recently for the separation of magnetically responsive calcite and aragonite microcrystals used as templates of the fabrication of cellosomes (9b), where the iron oxide nanoparticles were layerwise placed onto the polyelectrolyte-coated microparticles. Although effective, this approach utilizes the deposition of several polyelectrolyte layers prior to magnetization; therefore, it is time-consuming and, furthermore, polyelectrolytes may limit the potential applicability of LbL-modified magnetic microcrystals as sorbents because of nonspecific electrostatic adsorption, etc. Therefore, it is a challenge to produce magnetic calcium carbonate microcrystals via a single-step magnetization technique. In this Letter, we for the first time describe a simple approach for the fabrication of magnetically responsive $CaCO_3$ microcrystals by coprecipitation of calcite in the presence of citrate-stabilized iron oxide magnetic nanoparticles and demonstrate the use of these magnetic templates in the fabrication of hollow polyelectrolyte microcapsules.

RESULTS AND DISCUSSION

We synthesized calcium carbonate microcrystals doped with citric acid stabilized magnetic nanoparticles following a previously reported procedure that involves the coprecipitation of Ca^{2+} and CO_3^{2-} ions in aqueous media at room temperature for several days (2a). Normally, this approach yields the nucleation and subsequent growth of rhombohedral and polygonal colorless microcrystals with average sizes

* Corresponding author. Phone: +78432315246. E-mail: kazanbio@gmail.com.
Received for review June 3, 2009 and accepted August 18, 2009

DOI: 10.1021/am9003864

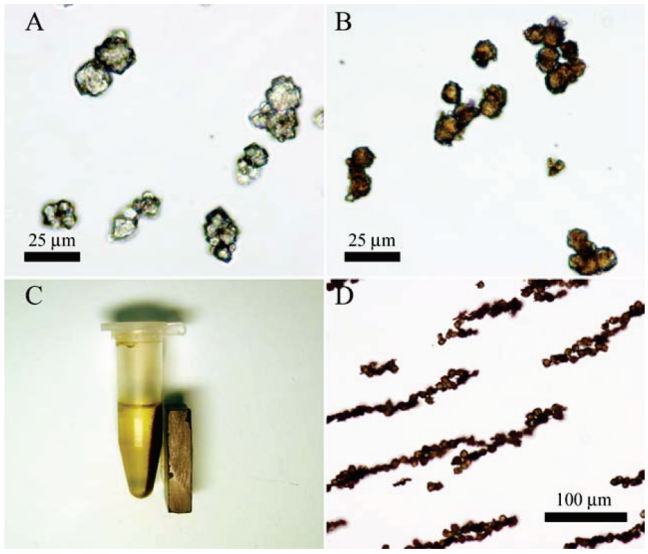

FIGURE 1. (a) Optical microscopy image of pristine calcium carbonate microcrystals (aqueous dispersion). (b) Optical microscopy images of calcium carbonate microcrystals doped with magnetic nanoparticles (aqueous dispersion). (c) Magnetic behavior of calcium carbonate microcrystals doped with magnetic nanoparticles induced by a permanent magnet. (d) Alignment of calcium carbonate microcrystals doped with magnetic nanoparticles in water along an external magnetic field.

of around 15 μm, which are presented in Figure 1A. In our modification of this method, in order to magnetically functionalize the calcium carbonate microcrystals, we used iron oxide nanoparticles, synthesized as described in ref 16, that had a mean particle size of 40 nm [as measured by dynamic light scattering (DLS), the size distribution diagram and the corresponding scanning electron microscopy (SEM) image of the magnetic nanoparticles are given in Figure S1 in the Supporting Information]. Nanoparticles were introduced at equal concentrations into both Ca^{2+} and CO_3^{2-} aqueous solutions prior to coprecipitation, and as a result, we obtained brownish polygonal microcrystals (Figure 1B–D) of similar sizes that were magnetically responsive if placed into an external magnetic field. As shown in Figure 1D, the microcrystals effectively align along the magnetic field and can be spatially manipulated and moved by a permanent magnet (see Movie 1 in the Supporting Information). It is worth noting that the magnetically responsive microcrystals immediately disassemble the long chains formed as a result of the external magnetic field if the permanent magnet is removed; thus, no magnetically induced aggregation happens in the suspensions of microcrystals.

SEM was used to investigate the structures of microcrystals synthesized in the presence and in the absence of magnetic nanoparticles, and the results are given in Figure 2. As one can see, both pristine microcrystals and microcrystals doped with magnetic nanoparticles are relatively large polyhedral microparticles (~10 μm), although several cubical microcrystals can be found as well. In contrast with pristine calcium carbonate, magnetically responsive $CaCO_3$ microcrystals contain magnetic nanoparticles, which can be clearly seen on the SEM images (Figure 2D). These nanoparticles incorporated into the crystalline structure of calcium carbonate provide the magnetic properties of an

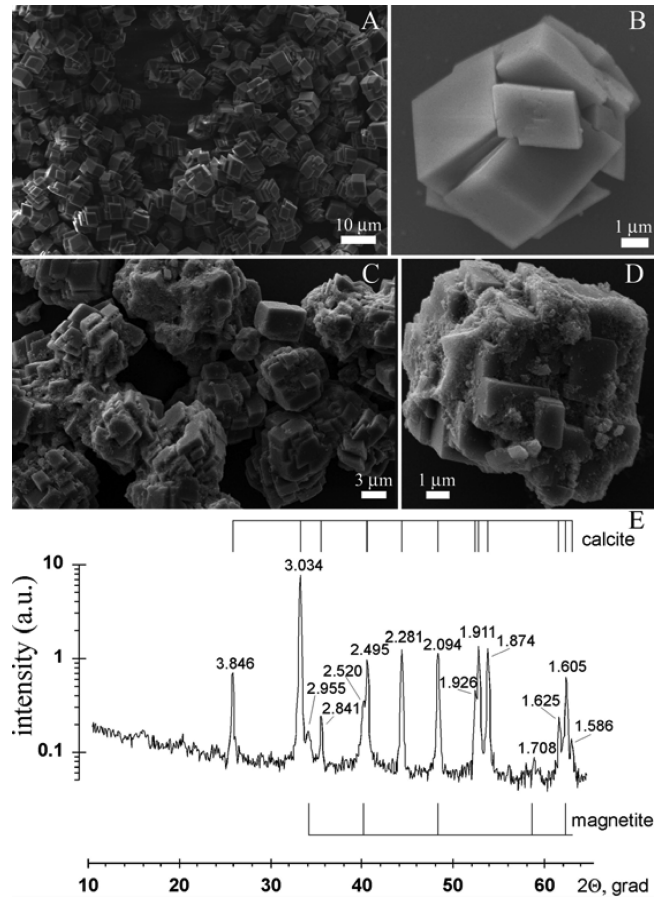

FIGURE 2. (a and b) SEM images of pristine calcium carbonate microcrystals. (c and d) SEM images of calcium carbonate microcrystals doped with magnetic nanoparticles. (e) Powder XRD pattern of calcium carbonate microcrystals doped with magnetic nanoparticles. The peaks originate from calcite and magnetite. The crystal lattice *d*-spacing values (Å) are given at the respective peaks.

originally nonmagnetic inorganic material and induce changes in color in comparison with pristine calcium carbonate. From the SEM images, we conclude that the nanoparticles are randomly distributed on the surface of the microcrystals and, possibly, inside the calcite microcrystals. The sizes and the rectangular appearance of the magnetically responsive microcrystals make them a versatile template for polyelectrolyte and microparticles deposition, while the magnetic properties introduced by magnetic nanoparticles allow for their convenient manipulation and magnetic separation.

The ability to manipulate the calcite microcrystals with an external magnetic field might be important in several applications, where even gentle low-speed centrifugation may severely damage assemblies based on the calcium carbonate microcrystals (i.e., if the crystals are used as templates for the fabrication of large multicellular or particulate assemblies (5)). Moreover, magnetically responsive calcite microcrystals can be utilized in microfluidic applications and microreactors in order to facilitate separation processes. In contrast with the conventional LbL assembly of magnetic nanoparticles onto calcium carbonate templates (5), the approach described here does not require time-consuming deposition/washing cycles.

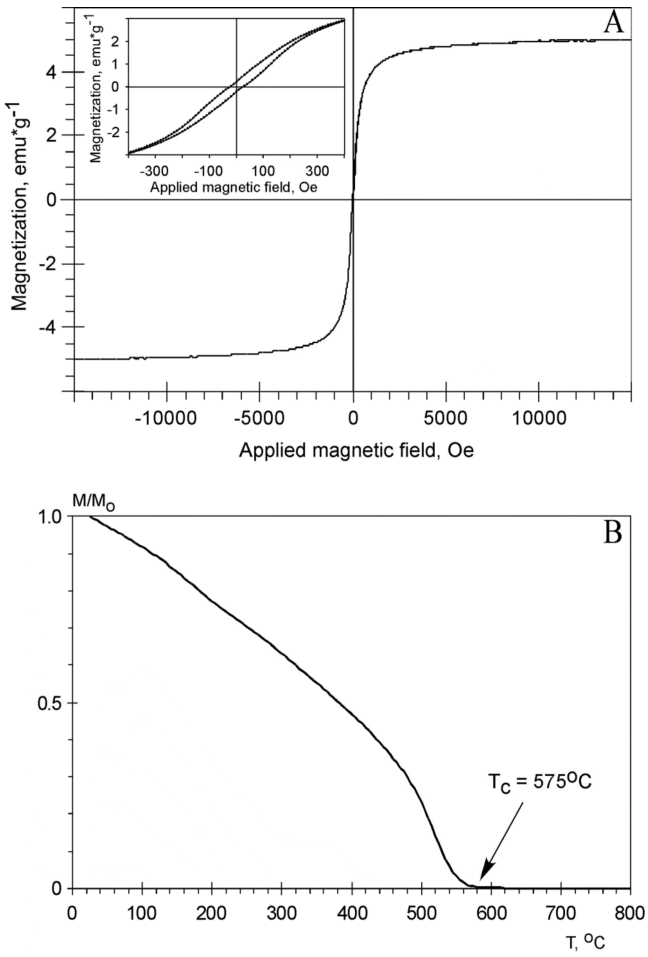

FIGURE 3. (a) Magnetization loop of calcium carbonate microcrystals doped with magnetic nanoparticles acquired at 300 K. The inset shows the hysteresis loop near the zero-magnetic-field region. (B) Thermomagnetic curve of calcium carbonate microcrystals doped with magnetic nanoparticles induced in a field of 2000 Oe. The arrow indicates the Curie temperature of magnetite.

The X-ray diffraction (XRD) spectrum of calcium carbonate rhombohedra doped with magnetic nanoparticles is given in Figure 2E. For referencing, we used the patterns of iron oxides and $CaCO_3$ isomorphs (calcite, aragonite, and vaterite) from the MINCRYST crystallographic database (17). We found that all of the peaks in the patterns obtained originate from calcite and magnetite. It should be noticed that the magnetite peaks (Figure 2E) are of very low intensity yet are clearly distinguishable.

The isothermal magnetization properties of calcite microcrystals doped with magnetic nanoparticles are presented in Figure 3A. We found that the saturation magnetization (M_s), saturation remanence magnetization (M_{rs}), and coercivity (H_c) were 4.99 emu g^{-1}, 0.51 emu g^{-1}, and 20 Oe, respectively. The inset in Figure 3A shows the hysteresis loop near the zero-magnetic-field region, and as one can see, the low values of M_{rs} and H_c indicate that the magnetic calcite microcrystals possess superparamagnetic properties. Further evidence of the superparamagnetic properties of magnetic microcrystals can be found from the relationship of the remanence magnetization value to the saturation magnetization value $M_{rs}/M_s = 0.102$, which is characteristic of the superparamagnetic behavior of single-domain nanoparticles (18). Furthermore, taking into account the fact that the saturation magnetization for calcite microcrystals doped with magnetic nanoparticles is 4.99 emu g^{-1}, which is much lower than that of bulk magnetite (92 emu g^{-1}) (19), we conclude that the low magnetization value is caused by the contribution of calcite as a nonmagnetic component in the total sample volume. These data suggest that the magnetite weight concentration in the sample is relatively small, apparently not exceeding 6% from the total mass of the bulk material, which is also suggested by the low intensities of the XRD peaks originating from magnetite.

Next, we investigated the thermomagnetic properties of calcite microcrystals doped with magnetic nanoparticles. Magnetization was induced in a field of 2000 Oe and measured as a function of the temperature (at a rate of 100 °C min^{-1}, in order to prevent the oxidation of magnetite nanoparticles, which would be obstructed at lower heating rates) until a sharp decrease of magnetization was detected (Figure 3B). As one can see, the thermomagnetic curve is characteristic of magnetite, which can be identified by the Curie temperature around 575 °C (20). As expected, the absence of inflection points indicates that no traces of other iron oxide species (i.e., hematite, maghemite, etc.) are present in calcite microcrystals doped with magnetic nanoparticles. It is worth noting that a uniform decrease of magnetization with increasing temperature suggests that the incorporated nanoparticles are of sizes less than the stable single-domain size dispersed as single-domain particles (21). As we demonstrate here, the thermomagnetic stability of magnetic calcite microcrystals up to 500 °C further widens the potential areas of use of this hybrid material.

In addition, as a proof-of-concept, we demonstrate the use of magnetically responsive calcite microcrystals as templates for the development of hollow polyelectrolyte microcapsules, using commercially available poly(allylamine hydrochloride) (PAH) and poly(sodium polystyrenesulfonate) (PSS) as materials for the fabrication of LbL polyelectrolyte shells (2). To demonstrate the integrity of the microcapsules by fluorescent microscopy, we used fluorescein isothiocyanate labeled PAH (FITC-PAH) as a component of polyelectrolyte films. Microcrystals were coated with several consecutive polyelectrolyte layers, resulting in the following shell architecture: PAH/PSS/PAH/PSS/FITC-PAH/PSS. After deposition of polyelectrolytes, calcite microcrystals were dissolved using 0.1 M HCl, yielding hollow cubiclike microcapsules, which, as one can see in Figure 4, retain their magnetic properties as a result of residual magnetic nanoparticles remaining in the microcapsules after dissolution of calcite cores. Because the iron oxide dissolution rates in acidic solutions are typically low (22), magnetite nanoparticles embedded in calcite cores remain stable after relatively short exposure to HCl LbL 1 h, whereas calcite microcrystals are dissolved (5).

The long chains of magnetically aligned microcapsules shown in Figure 4 are formed upon placement of a permanent magnet in the vicinity of the glass slide with a sample and disassemble almost immediately after the permanent

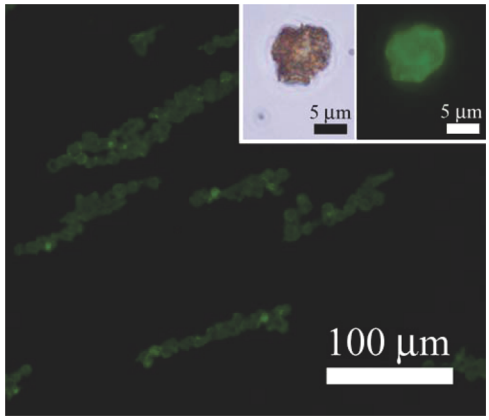

FIGURE 4. Fluorescent microscopy image of hollow polyelectrolyte microcapsules (shell architecture: PAH/PSS/PAH/PSS/FITC-PAH/PSS) aligned along an external magnetic field (the inset shows magnified optical and corresponding fluorescent microscopy images of a hollow microcapsule).

magnet is removed. Taking into account this fact, we suppose that magnetic manipulation can be used for the directed transportation or separation of these microcapsules while avoiding aggregation. As long as the microcapsules templated on sacrificial calcite microcrystals are magnetically responsive, they can be delivered or manipulated using an external magnet. The deposition of magnetite inside the calcite templates rather than the LbL coating of the microcrystals with nanoparticles (9b, 23) can be regarded as a simple one-step route of the magnetization of inorganic microparticles. In addition, if the magnetically responsive microcrocrystals are used as templates, there is no need for centrifugation of the samples, and separation of the particles might be performed using a relatively mild magnetic separation. Moreover, we suppose that residual amounts of magnetite in the microcapsules templated on magnetically responsive calcite microcrystals allow for the potential detection of microcapsules using magnetic resonance imaging (MRI) techniques (24). This will provide the materials based on calcite microcrystals doped with magnetic nanoparticles with a versatile tool for spatial manipulation and MRI-mediated tracking. In future work, it would be interesting to produce calcium carbonate microcrystals and amorphous microparticles of other (nonrhombohedral) shapes doped with magnetic nanoparticles.

To conclude, we synthesized a novel hybrid magnetically responsive material by coprecipitation of calcium carbonate rhombohedral microcrystals in the presence of citrate-stabilized iron oxide nanoparticles. XRD patterns indicate that the microcrystals obtained are made of calcite and magnetite. SEM studies reveal that the magnetic calcite microparticles have average sizes of 10 μm and the nanoparticles are assembled on the polygonal calcite microcrystals. The magnetic properties of the microcrystals obtained are characterized as superparamagnetic. In addition, we demonstrate the fabrication of hollow polyelectrolyte microcapsules templated on magnetically responsive calcite microcrystals, which retain their magnetic properties after decomposition of sacrificial cores and can be spatially manipulated using a permanent magnet. The simplicity of the approach described suggests that not only magnetic but also other metal nanoparticles can be similarly incorporated into calcite microcrystals; this work is currently performed in our group and will be reported in a follow-up paper. On the basis of our results, we expect a wide range of applications for these hybrid calcite microcrystals doped with magnetic nanoparticles.

EXPERIMENTAL SECTION

Synthesis of Magnetic Nanoparticles. Magnetic nanoparticles were synthesized as described in ref 16 with minor modifications. Briefly, 2.0 mL of 1 M $FeCl_3$ and 0.5 mL of 2 M $FeCl_2$ aqueous solutions were mixed, heated to 80 °C, and stirred vigorously. Then, 25 mL of a 1.0 M aqueous NH_3 solution was added dropwise with stirring; next, the brownish precipitate was separated using a permanent magnet and washed in Milli-Q water until neutral pH was detected. Then 25 mL of 0.1 M aqueous citric acid was added into the solution and sonicated for 10 min, resulting in the formation of a stable suspension of magnetic nanoparticles. Further, the nanoparticles obtained were filtered through 0.22 μm filters (Millipore). For the size distribution measurements of the nanoparticles, we performed DLS measurements using a Malvern Zetasizer Nano ZS at 25 °C. The Nano ZS contains a 4 mW He−Ne laser operating at a wavelength of 633 nm and an avalanche photodiode detector.

Synthesis of Magnetically Responsive Calcium Carbonate Microcrystals. Calcite microcrystals doped with magnetic nanoparticles were synthesized by mixing equal volumes of aqueous 0.33 M $CaCl_2$ and Na_2CO_3 in the presence of citrate-stabilized magnetic nanoparticles added before mixing (at a concentration of 50 mg mL^{-1}) at room temperature. The mixture was stirred briefly and left undisturbed for 4 days, and then the microcrystals were collected and dried at 70 °C for 30 min. Nonmagnetic calcite microcrystals were synthesized similarly by mixing aqueous 0.33 M $CaCl_2$ and $NaCO_3$ in the absence of magnetic nanoparticles (2a). After drying, the microcrystals were redispersed in water, if necessary.

Fabrication of LbL Polyelectrolyte Microcapsules Templated on Magnetically Responsive Calcium Carbonate Microcrystals. Calcite microcrystals doped with magnetic nanoparticles (aqueous dispersion, 20 mg mL^{-1}) were LbL-coated with several layers of oppositely charged polyelectrolytes, poly(allylamine hydrochloride) (PAH; M_w = 15 000 Da) and poly(sodium polystyrenesulfonate) (PSS; M_w = 70 000 Da) (Sigma-Aldrich), which were dissolved at a concentration of 5 mg mL^{-1} in 0.5 M NaCl by the introduction of 300 μL of an aqueous suspension of magnetic calcite into a PAH solution (incubation at room temperature for 15 min), followed by magnetic separation and washing three times with Milli-Q water. Next, the procedure was repeated using a PSS solution and then PAH, until the desired number of coatings were deposited onto the surfaces of the magnetic microcrystals. In order to demonstrate the integrity of the polyelectrolyte shells, FITC-PAH (Sigma-Aldrich; at a concentration of 0.5 mg mL^{-1} in 0.5 M NaCl) was used instead of PAH (the final shell architecture was PAH/PSS/PAH/PSS/FITC-PAH/PSS). To produce hollow polyelectrolyte microcapsules from the polyelectrolyte-coated magnetic calcite crystals, aqueous 0.1 M HCl was used to dissolve calcite microcrystals; the incubation time was 1 h.

Characterization Techniques. Optical and fluorescent microscopy images were taken using a Leica DMIL microscope equipped with a Leica DFC 290 CCD camera. SEM images were taken using a Carl Zeiss EVO 40 scanning electron microscope. Sample preparation for SEM was performed by placing 5 μL of a sample onto glass-coated microscopy stubs, drying overnight at 37 °C, and sputter-coating with a 10-nm-thick gold layer. The sizes of the microcrystals were calculated from SEM images

using *ImageJ* free software (25). XRD spectra were obtained using a Dron 2 (RF) powder X-ray diffractometer. The magnetic hysteresis loop of the samples was measured at 300 K using a homemade coercivity spectrometer described in detail in ref 26. Thermomagnetic properties were studied using a homemade magnetic Curie balance (27).

Acknowledgment. We gratefully acknowledge help from Prof. Dr. F. Şahin and M. Kahraman (Yeditepe University, Istanbul, Turkey), Dr. V. N. Paunov (The University of Hull, Hull, England), Prof. Dr. A. P. Kiyasov (Kazan State Medical University, Kazan, Republic of Tatarstan), Y. Osin (Kazan Physical-Technical Institute, Kazan, Republic of Tatarstan), and Dr. Vladimir P. Morozov, Alsu I. Zamaleeva, and Vadim S. Gavrilov (Kazan State University, Kazan, Republic of Tatarstan).

Supporting Information Available: A movie illustrating the magnetic behavior of calcite microcrystals doped with magnetic nanoparticles upon application of a permanent magnet and characterization of citric acid stabilized magnetic nanoparticles by SEM and DLS. This material is available free of charge via the Internet at http://pubs.acs.org.

REFERENCES AND NOTES

(1) (a) Hall, S. R.; Bolger, H.; Mann, S. *Chem. Commun.* **2003**, 2784–2785. (b) Wang, Y.; Liu, Z.; Han, B.; Huang, Y.; Yang, G. *Langmuir* **2005**, *21*, 10846–10849. (c) Xia, F.; Jiang, L. *Adv. Mater.* **2008**, *9999*, 1–17.

(2) (a) Holt, B.; Lam, R.; Meldrum, F. C.; Stoyanov, S. D.; Paunov, V. N. *Soft Matter* **2007**, *3*, 188–190. (b) Andreeva, D. V.; Gorin, D. A.; Mohwald, H.; Sukhorukov, G. B. *Langmuir* **2007**, *23*, 9031–9036.

(3) Petrov, A. I.; Volodkin, D. V.; Sukhorukov, G. B. *Biotechnol. Prog.* **2005**, *21*, 918–925.

(4) (a) He, Y.; Li, T.; Yu, X.; Zhao, S.; Lu, J.; He, J. *Appl. Surf. Sci.* **2007**, *253*, 5320–5324. (b) Gong, J.; Zhou, Z.; Hu, X.; Wong, M.; Wong, K.; Du, Z. *ACS Appl. Mater. Interfaces* **2009**, *1*, 26–29.

(5) Fakhrullin, R. F.; Paunov, V. N. *Chem. Commun.* **2009**, 2511–2513.

(6) Dickinson, S. R.; McGrath, K. M. *Cryst. Growth Des.* **2004**, *4*, 1411–1418.

(7) (a) Aizenberg, J.; Lambert, G.; Addadi, L.; Weiner, S. *Adv. Mater.* **1996**, *8*, 222–226. (b) Aizenberg, J.; Lambert, G.; Weiner, S.; Addad, L. *J. Am. Chem. Soc.* **2002**, *124*, 32–39.

(8) (a) Sondi, I.; Salopek-Sondi, B. *Langmuir* **2005**, *21*, 8876–8882. (b) Voinescu, A. E.; Touraud, D.; Lecker, A.; Pfitzner, A.; Kunz, W.; Ninham, B. W. *Langmuir* **2007**, *23*, 12269–12274. (c) Butler, M. F.; Frith, W. J.; Rawlins, C.; Weaver, A. C.; Heppenstall-Butler, M. *Cryst. Growth Des.* **2009**, *9*, 534–545. (d) Lukeman, P. S.; Stevenson, M. L.; Seeman, N. C. *Cryst. Growth Des.* **2008**, *8*, 1200–1202.

(9) (a) Lian, B.; Hu, Q.; Chen, J.; Ji, J.; Tengon, H. H. *Geochim. Cosmochim. Acta* **2006**, *70*, 5522–5535. (b) Fakhrullin, R. F.; Minullina, R. T. *Langmuir* **2009**, *25*, 6617–6621.

(10) (a) Gaponik, N.; Radtchenko, I. L.; Sukhorukov, G. B.; Rogach, A. L. *Langmuir* **2004**, *20*, 1449–1452. (b) Sadasivan, S.; Sukhorukov, G. B. *J. Colloid Interface Sci.* **2006**, *304*, 437–441. (c) Kommareddi, N. S.; Tata, M.; John, V. T.; McPherson, G. L.; Herman, M. F. *Chem. Mater.* **1996**, *8*, 801–809. (d) Zhang, H.; Lai, G.; Han, D.; Yu, A. *Anal. Bioanal. Chem.* **2008**, *390*, 971–977.

(11) (a) Utsumi, S.; Urita, K.; Kanoh, H.; Yudasaka, M.; Suenaga, K.; Iijima, S.; Kaneko, K. *J. Phys. Chem. B* **2006**, *110*, 7165–7170. (b) Yu, M.; Urban, M. W. *J. Mater. Chem.* **2007**, *17*, 4644–4646.

(12) Cho, E. C.; Shim, J.; Lenn, K. E.; Kim, J.; Han, S. S. *ACS Appl. Mater. Interfaces* **2009**, *1*, 1159–1162.

(13) Bonini, M.; Lenz, S.; Giorgi, R.; Baglioni, P. *Langmuir* **2007**, *23*, 8681–8685.

(14) Wang, L.; Sun, J. *J. Mater. Chem.* **2008**, *18*, 4042–4049. Rubio-Retama, J.; Zafeiropoulos, N. E.; Serafinelli, C.; Rojas-Reyna, R.; Voit, B.; Cabarcos, E. L.; Stamm, M. *Langmuir* **2007**, *23*, 10280–10285.

(15) (a) Lattuada, M.; Hatton, T. A. *J. Am. Chem. Soc.* **2007**, *129*, 12878–12889. (b) Dyab, A. K. F.; Ozmen, M.; Ersoz, M.; Paunov, V. N. *J. Mater. Chem.* **2009**, *19*, 3475–3481. (c) Lee, S. H.; Liddell, C. M. *Small* **2009**, DOI: 10.1022/smll.200900135.

(16) Sahoo, Y.; Goodarzi, A.; Swihart, M. T.; Ohulchanskyy, T. Y.; Kaur, N.; Furlani, E. P.; Prasad, P. N. *J. Phys. Chem. B* **2005**, *109*, 3879–3885.

(17) http://database.iem.ac.ru/mincryst/.

(18) (a) Stoner, E. S.; Wolhfarth, E. P. *Philos. Trans. R. Soc. London, Ser. A.* **1948**, *240*, 599–642. (b) Schrefl, T.; Hrkac, G.; Suess, D.; Scholz, W.; Fidler, J. *J. Appl. Phys.* **2003**, *93*, 7041–7043.

(19) Yamaura, M.; Camilo, R. L.; Sampaio, L. C.; Macedo, M. A.; Nakamura, M.; Toma, H. E. *J. Magn. Magn. Mater.* **2004**, *279*, 210–217.

(20) Dunlop, D. J.; Ozdemir, O. *Rock Magnetism: Fundamentals and Frontiers*; Cambridge University Press: New York, 1997; p 573.

(21) Bean, C. P.; Livingston, J. D. *J. Appl. Phys.* **1959**, *30*, 120S–129S.

(22) Bjorklund, R. B.; Hedlund, J.; Carlsson, B. *Langmuir* **1999**, *15*, 494–499.

(23) Hu, S.; Tsai, C.; Liao, C.; Liu, D.; Chen, S. *Langmuir* **2008**, *24*, 11811–11818.

(24) Krejci, J.; Pachernik, J.; Hampl, A.; Dvorak, P. *Gen. Physiol. Biophys.* **2008**, *27*, 164–173.

(25) http://rsbweb.nih.gov/ij/.

(26) Jasonov, P. G.; Nurgaliev, D. K.; Burov, B. V.; Heller, F. *Geol. Carpathica* **1998**, *49*, 224–225.

(27) Nurgaliev, D.; Borisov, A.; Heller, F.; Burov, B.; Jasonov, P.; Khasanov, D.; Ibragimov, S. *Geophys. Res. Lett.* **1996**, *23*, 375–378.

AM9003864